Spectral Features

Stuart Samuel
Lawrence Berkeley National Laboratory

Abstract

Certain Type Ia supernova spectral features have theoretically been found to probe progenitor initial conditions. We introduce a model for the spectral features and determine the signal-to-noise necessary in the spectrum to measure the relevant parameters to the accuracy targeted by SNAP. Possible variations in the definition of spectral depth, width, and position for different choices of model are explored.

Preface

The results of this section are somewhat of a preliminary nature for several reasons: The detector design specifications have not been finalized and are subject to revision. The systematic analysis is based on only six supernova flux data sets; hence only a rough estimate of the systematic uncertainty is achieved. However, more data sets are expected to become publicly available within a year. Finally, the analysis of the CaII features as not available in time for this report.

Introduction

The spectrum of a supernova contains considerable information about the physics of the stellar explosion. This information is encoded in a subtle way that is gradually being unraveled. Certain features such as troughs and peaks in the supernova flux are associated with P-Cygni profile spectra of elements. By measuring the features, it is possible to constrain the initial conditions, the subsequent dynamics, and chemistry of the explosion. Current theoretical models of type Ia supernovae are able to provide approximate correlations between changes in the physical conditions and the peak luminosity (Höflich, Wheeler, & Thielemann, 1998).

Some quantities that can be deduced from spectral features are the speed of the different elements in the ejecta, the opacity of inner layers, the metallicity of the progenitor, the ^{56}Ni mass, and the distribution of the ^{56}Ni. These quantities are related to the dynamics of the explosion as follows: The speed of the ejecta is a measure of the kinetic energy of the explosion; the opacity affects the overall light curve shape; the metallicity of the progenitor plays a role in the character of the spectrum at early times; the ^{56}Ni mass is an indicator of the total luminosity; and the ^{56}Ni distribution leads to small distortions of the light curve shape in the early development stage.

Three parameters have been selected to characterize a feature: the location of the local minimum or maximum of the flux, the width of the structure, and the height/depth of the structure. Table 4.4 of the SNAP proposal dated December 15, 2000 provides the accuracy required to measure these three parameters so that the error in the magnitude at maximum luminosity is less than 0.02.

The character of the host galaxy affects in part the age, metallicity and certain other properties of the supernova progenitor. More specifically, luminosities, colors, morphology and location within the galaxy allow one to estimate certain initial stellar conditions. Table 4.6 of the SNAP proposal lists observables that one would like to measure to constrain the progenitor environment. With this information, it will be possible to divide type Ia supernovae into groups, such that each supernova member arises from a similar environment. Light curve stretches, rise times, tails and peaks also provide information about ^{56}Ni mass, ^{56}Ni distribution, kinetic energy, and opacity of the explosion; these correlations are outlined in Table 4.5 of the SNAP proposal. See Branch, Romanishin, & Baron (1996) for more details. In summary, by combining host galaxy properties and light curve measurements with supernova spectral features, one is able to determine more accurately the physics of the supernova and to monitor possible changes in population as a function of redshift.

It is easy to understand why feature locations correlate with the kinetic energy of the ejecta. Ejecta that are moving toward earth are slightly blue-shifted compared to ejecta that are moving away from earth. Thus spectral line locations are a measure of velocities of supernova elements.

Likewise, the width of a feature is determined in part by the variation in velocity of ejecta. Ejecta that are traveling perpendicular to the line of sight to the supernova are not blue shifted, while ejecta that are traveling at the earth or at an angle to the line of sight are. Thus spectral lines are blue shifted by differing amounts leading to a smearing of a line of approximately $(15,000 \text{ km/s})/c \approx 5\%$ in the rest frame. For the SiII feature near 6000 Å, this analysis predicts a width of about 300 Å, which is indeed roughly what is observed. Similarly, the width of the CaII feature near 4000 Å should be about 200 Å.

The depth or height of a feature correlates with optical depths. When more material is present (due to a wider or denser envelope) more absorption occurs for radiation passing through the ejecta and more emission arises for radiating elements. It has been argued and empirically shown that the ratio of heights of certain features is a luminosity indicator (Nugent et al., 1995). Recent analysis by Peter Nugent reported at the May 2001 SNAP workshop indicates that the SiII height ratio is a better luminosity indicator than the CaII height ratio. The SiII ratio might provide a "standard candle" method that is competitive with stretch.

The rest of this section determines how different uncertainties affect the determination of spectral feature parameters. The uncertainties considered here are (1) statistical errors due to the detector and backgrounds, (2) systematic errors due to imprecisions in the definitions of heights and widths, and (3) a linear bias of flux measurements, e.g. due to error in the calibration.

The Effects of Statistical Errors on Spectral Feature Parameters

The error bars on data arise from detector noise, backgrounds, and the source itself. The former are generated from dark currents i_{dark} and from readout noise $\delta_{readout}$. The sky and host galaxy are background sources. In addition, the accuracy of data measurements improves with the intensity of the supernova flux. These five contributions lead to the variance σ^2_{data} of a data point (pixel) that is approximately

$$\sigma^2_{data} = n_{images}\delta^2_{readout} + t_{obs}i_{dark} + t_{obs}\Delta\lambda(\mathcal{F}_{SN} + \mathcal{F}_{galaxy} + \mathcal{F}_{sky}) \quad ,$$

where t_{obs} is the total observation time in seconds, n_{images} is the number of exposures taken, $\Delta\lambda$ is the wavelength width in Angstroms of the bin of the data point, and $\mathcal{F}_{SN}$, $\mathcal{F}_{galaxy}$ and $\mathcal{F}_{sky}$ are fluxes of respectively the supernova, the host galaxy and the sky expressed in machine units, i.e., electrons per second per Angstrom of wavelength. For the HgCdTe detector, $i_{dark} = 0.017$ electrons per second and $\delta_{readout} = 6$ electrons. For the optical detector, $i_{dark} = 0.0013$ electrons per second and $\delta_{readout} = 4$ electrons. The signal in a bin in electron counts is $t_{obs}\mathcal{F}_{SN}\Delta\lambda$.

The signal to noise $t_{obs}\mathcal{F}_{SN}\Delta\lambda/\sigma_{data}$ is determined from the information in the above paragraph. The three fluxes $\mathcal{F}_{SN}$, $\mathcal{F}_{galaxy}$ and $\mathcal{F}_{sky}$ for SNAP are generated from simulations written by Alex Kim. Since these fluxes are subject to revision, the results presented below are preliminary. The errors on data points depend on four variables: t_{obs}, n_{images}, $\Delta\lambda$ and the redshift z of the supernova (because the supernova and galaxy fluxes vary in distance and are redshifted). Thus, the statistical uncertainty on supernova spectral parameters depends on these four parameters.

Briefly, the method used to determine the statistical errors in the heights and widths is as follows: After shifting the location of the minimum or maximum to the origin, a fit $f(\lambda)$ to the flux was done in a feature region of a template type Ia supernova. Then errors in data points were incorporated. Suppose new data points are generated by Monte Carlo within the specified errors. A fit of the form $af((\lambda - c)/b)$ can be performed to the new data where a, b, and c correspond to the height/depth, width, and wavelength position respectively. A common approach to determining this uncertainty is by Monte Carlo methods: simulated data is generated repeatedly and the variances in the output spectral parameters is recorded. Since the values of t_{obs}, n_{images} and $\Delta\lambda$ have not yet been fixed for SNAP, Monte Carlo runs would have to be performed for a range of these three parameters. This would involve considerable CPU time. The same is true for numerical packages that deal with this problem such as those contained in the CERN package MINUIT. Instead, we have used an efficient analytic approach that is described in an Appendix below.

Two features have been analyzed: SiIIr near 6135 Å and SiIIl near 5775 Å for a supernova with $z = 1.6$ at four days after peak luminosity as recommended by Peter Nugent in the 2001 SNAP Simulation Workshop. The studies of the features at CaIIr near 3930 Å and CaIIl near 3585 Å will be performed at a future date. According to the Peter Nugent at the 2001 SNAP workshop, the SiII region is more useful than the CaII region as a luminosity indicator.

We have generated results (i) keeping the binwidth and exposure time t_{exp} fixed while varying the total observation time t_{obs} ($t_{obs} = t_{exp}n_{images}$), (ii) keeping t_{obs} and n_{images} fixed while varying the bin width $\Delta\lambda$, and (iii) keeping t_{exp} and $\Delta\lambda$ fixed while varying n_{images} (and hence t_{obs}). Space limitations do not allow us to present all these results. The following represents typical uncertainties. They are generated for the case $\Delta\lambda/(1+z) \approx 10$ Å, and $t_{obs} \approx 20$ hours via ten exposures each of two hour duration ($n_{images} = 10$ and $t_{exp} = 2$ hours). Since we are not instrument noise limited, for case (i), the fractional errors go down

roughly as $1/\sqrt{t_{obs}\Delta\lambda}$. Errors also go down as the binwidth is made larger because the errors due to the detector are relatively smaller.

For SiIIr near 6135 Å, the uncertainties in height, width and location are respectively about 2.5%, 6.5% and 3.5 Å. For SiIIl near 5775 Å, results depend on whether the feature is deep or shallow and whether its shape is known. For some supernovae, the SiIIl feature is almost as pronounced as the one at 6135 Å. In this case, one can expect the uncertainties to be about the same as for the SiIIr case above. However, when the SiIIl feature is not very salient, then the uncertainties in height, width and location are respectively about 2%, 22% and 10 Å, if the shape of the feature is known. If the shape of the feature is not known, the uncertainty in measuring the height should be about 10%.

The following are two examples of simulated SNAP data of supernova features. The vertical axis represents supernova flux in arbitrary units. The horizontal axis is wavelength in Angstroms. Error bars were provided by Alex Kim under the assumption of ten exposures of two hours each (an observation of 20 hours total). Results are shown in the supernova rest frame by redshifting the wavelength by $(1+z) = 2.6$, and the experimental binwidth was 26 Å. The curves are fits to the data.

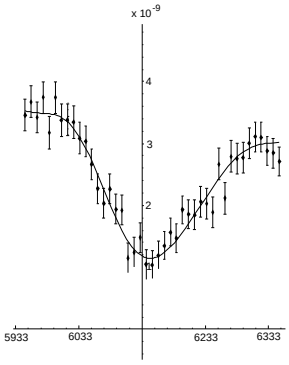

Figure 1. The SiII feature near 6125 Å. The statistical errors in the simulated data lead to values of the height, width and minimum location that are respectively 4% more, 4% more and 5 Å more than the case of perfect data with zero statistical errors.

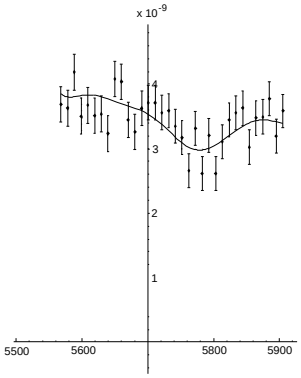

Figure 2. The SiIIl feature near 5775 Å for a shallow feature case. The statistical errors in the simulated data lead to values of the height, width and and maximum location that are respectively 0.2% lower, 14% lower and 0 Å more than the case of perfect data.

Two parameters of particular interest are the Silicon II ratio height R(SiII) and the Silicon II velocity V(SiII). They already have been observed to vary systematically in type Ia supernovae. The spectral requirements of a 0.02 magnitude uncertainty, which were provided by Peter Nugent in the 2001 SNAP Simulation Workshop, are that R(SiII) be accurate to 4% and that V(SiII) be accurate to 2000 km/s. Assuming no

intrinsic dispersion, the later translates into the requirement that the location error of the minimum be less than 40 Å, which is easily satisfied. The height of a single SiII feature should be measured to about 3%. For the case of a deep SiIIl feature, 10-hour exposures are needed. This corresponds to a signal-to-noise of roughly 12 in each 15Å pixel bin over the feature. For the case of a weak feature, it will be difficult to measure R(SiII) to the required accuracy unless SiIIl has a universal shape.

Systematic Effects

The above results might depend on the template type Ia supernova used for producing the fitting function f. The issue, here, is related to the problem of defining the height and width of a feature. Several reasonable definitions are possible. This leads to a systematic error in the feature parameters.

There is no standard method for determining this systematic error. The following is the way we approached the problem.

Let f_0 denote the original fitting function referred to as f above. Six additional type Ia supernova spectra were considered, and each was fit with a function f_i. These six fitting functions were scaled (shifted and stretched both horizontally and vertically) to match as best as possible the original fitting function f_0. Each of the six fitting functions was used to measure the height, width and location of the minimum/maximum by using the form $af_i((\lambda - c)/b)$ to fit five other data sets that are generated from the f_i at a wavelength interval of $\Delta\lambda$. The value of 10 Å was used for $\Delta\lambda$. The variations in a, b and c were noted and used to estimate the systematic uncertainty in height, width and location of the feature.

For heights, an additional method of estimating the systematic uncertainty was used. Two heights may be determined from each feature of a spectrum: the distance h_l from the minimum (or maximum) to the left shoulder and the distance h_r from the minimum (or maximum) to the right shoulder. The quantity $|h_l - h_r|/(h_l + h_r)$ when averaged over different spectra is a measure of the systematic uncertainty in height. Below we refer to this as the shoulder variation method.

The analysis was not done for the CaIIl peak near 3585 Å because not enough type Ia supernova data sets were available.

The following is a summary of the approximate systematic errors in height, width and location of the two features SiIIr near 6135 and CaIIr near 3930 Å.

For SiIIr near 6135 Å:
Systematic uncertainty in the location of the minimum is about 2.5 Å
Systematic uncertainty in width is about 6%
Systematic uncertainty in height is about 5%
Systematic uncertainty in height is about 5% using shoulder variation method

For CaIIr near 3930 Å:
Systematic uncertainty in the location of the minimum is about 2 Å
Systematic uncertainty in width is about 12%
Systematic uncertainty in height is about 24%
Systematic uncertainty in height is about 28% using shoulder variation method

A number of things are worth commenting on: (a) There is little systematic uncertainty in the minima/maxima locations, as one might expect: there is little ambiguity in what one means by a minimum or maximum. (b) The large uncertainty in the feature CaIIr near 3930 Å arises because the feature appears on a "steep slope". (c) The systematic uncertainty of the SiIIr heights are the order of 5%. This is approximately the same variation as seen by Peter Nugent and collaborators in using the SiII height ratio as a luminosity indicator. (d) If the systematic uncertainty in the SiII height ratio is 5%, one cannot expect it to be used more accurately as a luminosity indicator. It is possible that a more accurate luminosity indicator is "buried" in the feature and that the height ratio only approximates it. It is also possible that the height ratio is the best luminosity feature indicator but has an intrinsic uncertainty of about 5%. (e) The function fitting method and the shoulder variation method are in agreement. (f) Since seven spectral data sets is not a large sample, the above results should be regarded as preliminary.

Effects of a Linear Bias on Spectral Feature Measurements

In this section, we examine the effect of a possible linear calibration bias. If $flux_{true}$ and $flux_{outputted}$ are respectively the true supernova flux and the calibrated output flux, then the error in the measured flux

is

$$\delta flux = flux_{true} - flux_{outputted} \approx \alpha + \beta * \lambda \quad ,$$

where α and β are small coefficients characterizing the bias and λ is the wavelength. SNAP aims to calibrate the detector with sufficient accuracy so that the linear bias will be less than about 1% per 10,000 Å.

The bias affects the measurements of the parameters characterizing spectral features. It is straightforward to determine the distortion of the height, width and location of a feature caused by α and β. Constraints on the measured accuracy of feature parameters are provided in Table 4.4 of the SNAP proposal dated December 15, 2000.

It turns out that these constraints lead to the requirement that β be less than a few percent per 100 Å. This is about 100 times less stringent than SNAP design goals (which were chosen for other criteria). Thus, a linear bias at the designed level will not affect the determination of spectral-feature parameters.

Appendix: An Analytic Method of Determining the Variances in Fitting Parameters that Arise from Error Uncertainties in Data

Suppose $\{x_i, y_i\}$ for $i = 1, 2, \ldots, N_{data}$ are the expected "perfect" data points from some planned experiment. In the real experiment, errors associated with the data will arise. Suppose $f(x_i, a_r)$ is a function that fits the data ($f(x_i, a_r) \approx y_i$) and that depends on a set of parameters a_r, $r = 1, 2, \ldots, N_{parameters}$. These parameters could be important outputs that the experiment would like to measure accurately. The error uncertainties in data lead to uncertainties in the output parameters a_r. One is interested in determining the error bars for the a_r.

A standard way to proceed is by Monte Carlo methods, that is, to generate lots of simulated data and to examine the variation in the output parameters. This is a straightforward approach that involves the writing of computer programs and performing the number-crunching.

Due to machine design issues and future technological improvements, the values of the errors may change. In such a case, a Monte Carlo run must be performed for each case. Depending on the number of different situations, considerable computer time and programming may be needed.

In the analysis of the SNAP spectral features, we have used a more efficient analytic approach that is described in this Appendix. If the data errors are sufficiently small, the variance $\sigma_{a_r}^2$ is linearly dependent on the variances σ_i^2 of the data:

$$\sigma_{a_r}^2 = \sum_{i=1}^{N_{data}} C_{a_r}^i \sigma_i^2 + \ldots \quad ,$$

where $+\ldots$ indicates terms of order σ_i^4 or higher (σ_i^3 or higher if the error distribution is skewed). If the coefficients $C_{a_r}^i$ can be determined then the errors in output parameters can be readily computed.

The analytic approach has the following advantages over the Monte Carlo method:
(1) It can involve considerably less computer time.
(2) No testing for convergence of the simulation is needed.
(3) Examination of the coefficients $C_{a_r}^i$ allows one to determine where to concentrate one's experimental efforts to minimize the errors in output parameters.
(4) The method works for arbitrary data error distributions $P_i(\epsilon_i)$.

The disadvantages of the analytic approach compared to the Monte Carlo method are:
(1) The formulas for the coefficients $C_{a_r}^i$ become complicated as the number of parameters $N_{parameters}$ increases.
(2) The method is inaccurate if the error bars on the data are large (i.e., the terms omitted in the above equation of $\sigma_{a_r}^2$ are important). However, if the error bars are so large as to render the analytic method ineffective, one should probably rethink how the experiment is conducted.

The analytic approach has connections with imaginary-time Feynman path integrals that are used in quantum mechanics and field theory. Indeed, a discrete functional integral arises. Suppose the experimental data points y_i^{exp} are related multiplicatively to ideal data points y_i by

$$y_i^{exp} = y_i(1 + \epsilon_i) \quad .$$

Then the measure for the errors is

$$\prod_{i=1}^{N_{data}} P_i(\epsilon_i) d\epsilon_i \quad .$$

If the data error distributions $P_i(\epsilon_i)$ are normally distributed, then a Gaussian functional integral arises. In terms of the Monte Carlo approach, each simulation run corresponds to a path of the Euclidean functional integral.

The error distribution functions satisfy

$$\int_{-\infty}^{\infty} d\epsilon_i \, P(i, \epsilon_i) = 1 \quad ,$$

$$\int_{-\infty}^{\infty} d\epsilon_i \, P(i, \epsilon_i) \epsilon_i = 0 \quad ,$$

$$\int_{-\infty}^{\infty} d\epsilon_i \, P(i, \epsilon_i) \epsilon_i^2 = \sigma_i^2 \quad ,$$

and it is assumed that there are no correlations between different data points, that is, $P(\epsilon_i, \epsilon_j) = P(i, \epsilon_i) \, P(j, \epsilon_j)$ so that

$$\int_{-\infty}^{\infty} d\epsilon_i d\epsilon_j P(\epsilon_i, \epsilon_j) \epsilon_i \epsilon_j = 0 \quad .$$

This is often the case because statistical errors for different data points are independent. It is possible to modify the formulas for cases for which error-data correlations exist, but this is not done here.

Here is a derivation of the variance coefficients C_a^i for the one parameter case. The fitting function $f(x, a)$ depends on a single parameter a. Let a_0 be the best fit for a for perfect data; a_0 is determined by minimizing the chi-squared fit*

$$\chi^2(a) = \sum_{i=i}^{N_{data}} \left(f(x_i, a) - y_i \right)^2 \quad ,$$

that is,

$$\left. \frac{\partial \chi^2(a)}{\partial a} \right|_{a_0} = 0 = 2 \sum_{i=i}^{N_{data}} \left(f(x_i, a_0) - y_i \right) \frac{\partial f(x_i, a_o)}{\partial a} \quad .$$

If $f(x, a_0)$ is a perfect fit, then $\chi(a_0) = 0$ and $f(x_i, a_0) = y_i$.

When errors ϵ_i are introduced for the ith data point, the measured value y_i^{exp} of the ith data point may deviate from the ideal value of y_i. In what follows, we assume multiplicative errors ($y_i^{exp} = y_i(1 + \epsilon_i)$). The methods works for additive errors or a combination of both additive and multiplicative errors. See the discussion below.

The fitting of the parameter a using experimental data is determined by requiring that the chi-square fit

$$\chi^2(a, \{\varepsilon_j\}) = \sum_{i=i}^{N_{data}} \left(f(x_i, a) - y_i (1 + \varepsilon_i) \right)^2$$

be minimized:

$$\left. \frac{\partial \chi^2(a, \{\varepsilon_j\})}{\partial a} \right|_{a_s(\{\varepsilon_j\})} = 0 = 2 \sum_{i=i}^{N_{data}} \left(f(x_i, a_s(\{\varepsilon_j\})) - y_i (1 + \varepsilon_i) \right) \left. \frac{\partial f(x, a)}{\partial a} \right|_{a = a_s(\{\varepsilon_j\})} \quad .$$

* The least squares sum is employed without summands being divided by σ_i^2 because the original supernova flux data had negligible errors. It is straightforward to obtain formulas for the case when $1/\sigma_i^2$ factors are present: One replaces $y_i \to y_i/\sigma_i$ and $f(x_i) \to f(x_i)/\sigma_i$ in the equations.

Here, a_s is the minimizing solution. As long as the errors ϵ_i are small, one may expand about the perfect data case:

$$a_s\left(\{\varepsilon_k\}\right) = a_0 + \sum_i \varepsilon_i \left.\frac{\partial a_s}{\partial \varepsilon_i}\right|_{\{\varepsilon_k=0\}} + \frac{1}{2}\sum_{i,j}\varepsilon_i\varepsilon_j \left.\frac{\partial^2 a_s}{\partial\varepsilon_i\partial\varepsilon_j}\right|_{\{\varepsilon_k=0\}} + \ldots \quad .$$

Then it is straightforward to show that the variance in a is

$$\left\langle a^2\right\rangle - \left\langle a\right\rangle^2 = \sum_{i=i}^{N_{data}} \sigma_i^2 \left(\left.\frac{\partial a_s}{\partial\varepsilon_i}\right|_{\{\varepsilon_k=0\}}\right)^2 + \ldots \quad .$$

Define

$$A \equiv \frac{1}{2}\left.\frac{\partial^2\chi^2\left(a\right)}{\partial a^2}\right|_{a=a_s,\{\varepsilon_k=0\}} \quad ,$$

$$B_i \equiv -\frac{1}{2}\left.\frac{\partial^2\chi^2\left(a\right)}{\partial a\partial\varepsilon_i}\right|_{a=a_s,\{\varepsilon_k=0\}} \quad .$$

Then the small ϵ_i expansion leads to the following formula

$$\sigma_a^2 \equiv \left\langle a^2\right\rangle - \left\langle a\right\rangle^2 = \frac{1}{A^2}\sum_{i=i}^{N_{data}} \sigma_i^2 B_i^2 + \ldots \quad .$$

The quantities A and B_i can be evaluated in terms of the fitting function $f(x,a)$ and the data (x_i, y_i):

$$A = \sum_{i=i}^{N_{data}} \left[\left(\frac{\partial f\left(x_i,a_o\right)}{\partial a}\right)^2 + \left(f\left(x_i,a_o\right) - y_i\right)\frac{\partial^2 f\left(x_i,a_o\right)}{\partial a^2}\right] \quad ,$$

$$B = y_i \frac{\partial f\left(x_i,a_o\right)}{\partial a} \quad .$$

Usually, the second term in A can be neglected because the fit is good. If this is not the case, one should probably do a better job of obtaining $f(x,a)$. With a good fit, B may be replaced by

$$B = f\left(x_i,a_o\right)\frac{\partial f\left(x_i,a_o\right)}{\partial a} \quad ,$$

and the variance in a is determined completely by the fitting function and the location x_i of the data.

Supernova spectral features consist of emission-spectrum peaks and absorption-spectrum troughs. They are characterized by three parameters: the location of a minimum or maximum, the height of the feature and the width of the feature.

The analytic method for three parameters (a, b and c) is evaluated using the following formulas. The variances and cross variances in the parameters are

$$\sigma_{p_1p_2}^2 = \frac{1}{\Delta^2}\sum_{i=i}^{N_{data}} \sigma_i^2 B_i^{p_1} B_i^{p_2} + \ldots \quad ,$$

where p_1 and p_2 stand for either a, b or c, and where

$$\Delta = \det\begin{pmatrix} S_{f_a^2} & S_{f_af_b} & S_{f_af_c} \\ S_{f_bf_a} & S_{f_b^2} & S_{f_bf_c} \\ S_{f_cf_a} & S_{f_cf_b} & S_{f_c^2} \end{pmatrix} \quad ,$$

$$B_i^a = y_i \det\begin{pmatrix} \frac{\partial f\left(x_i,a_o,b_o,c_o\right)}{\partial a} & \frac{\partial f\left(x_i,a_o,b_o,c_o\right)}{\partial b} & \frac{\partial f\left(x_i,a_o,b_o,c_o\right)}{\partial c} \\ S_{f_bf_a} & S_{f_b^2} & S_{f_bf_c} \\ S_{f_cf_a} & S_{f_cf_b} & S_{f_c^2} \end{pmatrix} \quad ,$$

$$B_i^b = y_i \det \begin{pmatrix} S_{f_a^2} & S_{f_a f_b} & S_{f_a f_c} \\ \frac{\partial f(x_i,a_o,b_o,c_o)}{\partial a} & \frac{\partial f(x_i,a_o,b_o,c_o)}{\partial b} & \frac{\partial f(x_i,a_o,b_o,c_o)}{\partial c} \\ S_{f_c f_a} & S_{f_c f_b} & S_{f_c^2} \end{pmatrix} \quad ,$$

$$B_i^c = y_i \det \begin{pmatrix} S_{f_a^2} & S_{f_a f_b} & S_{f_a f_c} \\ S_{f_b f_a} & S_{f_b^2} & S_{f_b f_c} \\ \frac{\partial f(x_i,a_o,b_o,c_o)}{\partial a} & \frac{\partial f(x_i,a_o,b_o,c_o)}{\partial b} & \frac{\partial f(x_i,a_o,b_o,c_o)}{\partial c} \end{pmatrix} \quad .$$

The sums appearing in these equations are

$$S_{f_{p1} f_{p2}} = \sum_{i=i}^{N_{data}} \left[\frac{\partial f\left(x_i, a_o, b_o, c_o\right)}{\partial p_1} \frac{\partial f\left(x_i, a_o, b_o, c_o\right)}{\partial p_2} + \left(f\left(x_i, a_o, b_o, c_o\right) - y_i\right) \frac{\partial^2 f\left(x_i, a_o, b_o, c_o\right)}{\partial p_1 \partial p_2} \right] \quad .$$

These results follow from the first order dependencies of the parameters on data errors:

$$\left. \frac{\partial p_1}{\partial \varepsilon_i} \right|_{\{\varepsilon_k = 0\}} = \frac{B_i^{p_1}}{\Delta} \quad .$$

It is obvious from the form of the equations for the three-parameter case as to how to obtain the formulas for an arbitrary number of parameters. If the errors are additive instead of multiplicative then the factors of y_i in the B_i are absent.

Two checks of the equations were performed. For a linear fit $f(x, a, b) = a + bx$, it is possible to show that the formalism reduces to results given in Section 14.2 of "Numerical Recipes: The Art of Scientific Computing" (Cambridge University Press, 1986). For the three parameter case, a Monte Carlo simulation was performed to numerically verify the equations.

Bibliography

Branch, D., Romanishin, W. & Baron, E. (1996), ApJ, 465, 73.

Höflich, P., Wheeler, J.C, & Thielemann, F. K. (1998), ApJ, 495, 617.

Nugent, P. and Phillips, M. and Baron, E. and Branch, D. and Hauschildt, P. (1995), ApJ, 455, L147.

Press, W. H. (1986) "Numerical recipes : the art of scientific computing", Cambridge ; New York : Cambridge University Press.